Journal of Inflammation Research

Dovepress
Taylor & Francis Group

Open Access Full Text Article

ORIGINAL RESEARCH

Melatonin Activates KEAP1/NRF2/PTGS2 Pathway to Attenuate Hyperoxia-Driven Ferroptosis in Bronchopulmonary Dysplasia

Xianhui Deng[1,2,*], Anni Xie[2,*], Danni Ye[2], Yizhe Ma[1], Zhidan Bao[1], Qiuyan Xie[2], Zichen Luo[2], Ran Wang[2], Hu Li[1], Renqiang Yu[2]

[1]Department of Neonatology, Jiangyin People's Hospital, Wuxi, People's Republic of China; [2]Department of Neonatology, Affiliated Women's Hospital of Jiangnan University, Wuxi Maternity and Child Health Care Hospital, Wuxi, People's Republic of China

*These authors contributed equally to this work

Correspondence: Hu Li; Renqiang Yu, Email 1509503239@qq.com; yurenqiang553@163.com

Background and Purposes: Ferroptosis, a type of regulated cell death, has been confirmed to play a role in the pathogenesis of bronchopulmonary dysplasia (BPD). This study aimed to test the hypothesis that melatonin mitigates hyperoxia-induced BPD by inhibiting ferroptosis in alveolar epithelial cells, specifically through modulation of the KEAP1/NRF2/PTGS2 signaling pathway.

Methods: Hyperoxia-induced MLE-12 cells and neonatal mice were used to establish BPD models. The effects of melatonin on hyperoxia-induced ferroptosis in MLE-12 cells were assessed by administering melatonin and ferroptosis inducer erastin to these cells. Key target genes involved in melatonin's ameliorative effects on BPD were identified using bioinformatics analysis. To confirm the regulatory relationship between melatonin and the KEAP1/NRF2/PTGS2 pathway, MLE-12 cells were treated with the NRF2 inhibitor ML385 under hyperoxic conditions. Additionally, molecular docking was performed to predict interactions between melatonin and KEAP1.

Results: Melatonin (MT) treatment up-regulated the expression of glutathione peroxidase 4 (GPX4) and xCT in hyperoxia-treated alveolar epithelial cells. The anti-ferroptosis effect of MT on these cells was significantly reduced by ML385, confirming the role of the KEAP1/NRF2 pathway in MT's mechanism of action. In vivo experiments demonstrated that MT up-regulated NRF2, GPX4, and xCT levels and down-regulated KEAP1 and PTGS2 levels in hyperoxia-induced BPD models.

Conclusion: Melatonin exerts a protective effect against hyperoxia-induced BPD by inhibiting ferroptosis in alveolar epithelial cells, and this effect is mediated, at least in part, through the KEAP1/NRF2/PTGS2 axis.

Keywords: bronchopulmonary dysplasia, ferroptosis, melatonin, KEAP1, NRF2, PTGS2

Introduction

Bronchopulmonary dysplasia (BPD), a respiratory disorder predominantly affecting preterm infants, is characterized by alveolar simplification and arrested vascular development.[1,2] The pathogenesis of BPD involves multifactorial mechanisms, including hyperoxia-induced toxicity, inflammatory insults, and prematurity-related immaturity, with inflammation being a predominant etiological driver.[3,4] Current clinical management lacks definitive therapies and primarily relies on supportive strategies such as vitamin A supplementation, glucocorticoids, and mechanical ventilation.[5–7] Consequently, many infants with BPD face significant challenges during recovery, exhibiting high in-hospital mortality rates. Identifying effective therapeutic interventions is thus critical for improving outcomes in this population.

Alveolar epithelial cells synthesize surfactant protein C (SPC), which facilitates repair of damaged alveolar epithelium.[8] Preterm infants exhibit inherent pulmonary immaturity at birth, including insufficient surfactant production, underscoring the necessity of protecting alveolar epithelial cells. While oxygen therapy remains a cornerstone respiratory support for preterm infants, prolonged hyperoxia exacerbates lung injury, particularly in pulmonary epithelial cells,

Received: 4 March 2025
Accepted: 31 May 2025
Published: 11 June 2025

ultimately contributing to BPD pathogenesis.[9] Studies suggest that surfactant replacement therapy in preterm neonates reduces major complications and hospitalization rates.[10]

Ferroptosis, a novel form of regulated cell death, is driven by intracellular Fe^{2+} overload. Excessive Fe^{2+} catalyzes the Fenton and Haber-Weiss reactions, generating highly toxic reactive oxygen species (ROS) that induce lipid peroxidation and ferroptosis.[11] Key regulators of ferroptosis include glutathione peroxidase 4 (GPX4), ferritin heavy chain 1 (FTH1), and solute carrier family 7 member 11 (SLC7A11) also known as xCT.[12] Emerging evidence implicates ferroptosis in BPD pathogenesis, where activation of the nuclear factor erythroid 2-related factor 2 (NRF2)/heme oxygenase-1 (HO-1) axis suppresses alveolar epithelial ferroptosis, ameliorating lung injury.[13–15] Upon oxidative stress, Kelch-like ECH-associated protein-1 (KEAP1) dissociates from NRF2, enabling NRF2 nuclear translocation and subsequent binding to antioxidant response elements (ARE) to activate cytoprotective transcription. Our prior work established the pivotal role of NRF2 in BPD progression.[16]

Melatonin (MT), a hormone primarily secreted by the pineal gland, regulates circadian rhythms, sleep-wake cycles, immune responses, and exhibits potent anti-inflammatory and antioxidant properties.[17,18] Extensive studies identify MT as a robust natural antioxidant that enhances tissue antioxidant capacity by upregulating enzymes such as superoxide dismutase (SOD) and GPX.[19] MT has demonstrated ferroptosis-suppressive effects in diverse pathologies, including acute kidney injury, acute respiratory distress syndrome (ARDS), traumatic brain injury, and myocardial injury.[20–23] Recent investigations confirm MT's therapeutic potential in BPD, though its mechanistic underpinnings remain elusive.[24–27] However, whether MT alleviates BPD by inhibiting pulmonary epithelial ferroptosis remains unexplored.

In this study, we investigate whether MT mitigates BPD through ferroptosis inhibition in vitro and in vivo, and elucidate the underlying molecular mechanisms. Our findings may provide novel therapeutic strategies for BPD management.

Methods

Animal Treatment

The C57BL/6J wild pregnant female mice were developed in Jiangnan University (Wuxi), Jiangsu Province. Experimental procedures were approved by the Experimental Animal Care and Use Committee of Jiangnan University (JN.No20240315c0180630[108]) and the Guide for the Care and Use of Laboratory Animal published by the US National Institutes of Health (NIH publication, Eighth edition, 2011).

Animal Model and Study Design

The animal model and research design employed a murine model of bronchopulmonary dysplasia (BPD) induced by hyperoxia. Briefly, neonatal mice within 12 hours of birth were randomly assigned to four groups: control group(CON), control + melatonin group(MT), hyperoxia group(HYP), and hyperoxia + melatonin group(HYP+MT). Melatonin (10 mg/kg)[28] was administered via intraperitoneal injection daily for 7 consecutive days starting from postnatal day 7 until postnatal day 14, when body weights were measured and lung tissues were collected.

Pathological Examination of the Lung Tissues

The mice were anesthetized, and the left lung lobes were collected, soaked in 10% formalin buffer, and embedded in paraffin. Lung tissue slices with a thickness of 3 μm were taken. The morphology of lung injury was observed by hematoxylin-eosin (HE) staining. The radial alveolar number (RAC) and mean linear intercept (MLI) were calculated according to previous reports. To determine the immunoreactivity of ferroptosis marker protein GPX4, lung tissue sections were immunostained, followed by detection of avidin-biotin complex signal with biotinylated secondary antibody and 3,3′-diaminobenzidine (DAB) solution.

Immunofluorescence Staining

MLE-12 cells was seeded in Petri dishes at a density of 1×10^5 cells /mL. After 24 h, the cells were immersed in 4% paraformaldehyde for 15 min and 0.5% Triton X-100 for 20 min at room temperature. They were then washed three times

with phosphate buffer (PBS) and then incubated with 3% bovine serum albumin (BSA) for 30 min at room temperature. Primary antibody was then added overnight at 4 °C (1:400 dilution of 1% BSA in PBS). Cells were washed three times with cold PBS and then incubated in Alexa 488-labeled secondary antibodies. The cells were stained with 1 mg/mL DAPI solution for 5 min at room temperature. After the slides were washed again, images were acquired on a zeiss upright microscope (Carl Zeiss, Germany).Mice were anesthetized, and the left lung lobes were collected, soaked in 10% formalin buffer, and embedded in paraffin. Lung tissue sections with a thickness of 3 μm were taken. The procedure was the same as for cell fluorescent staining.

Cell Culture and Treatment

MLE-12 cells were obtained from ScienCell (Carlsbad, CA) and cultured in endothelial cell medium (ECM) containing fetal calf serum, antibiotics, and endothelial cell growth serum in a humidified atmosphere at 37 °C and 5% CO_2 as recommended by the manufacturer (Scien Cell). The normal group was 37 °C, 21% normoxic environment. The treatment group was pretreated with 10μM melatonin and incubated at 37 °C for 2 h,[29] and then placed in 85% hyperoxia for 24 h before the samples were collected.

Real-Time Quantitative Polymerase Chain Reaction (qPCR)

Lung tissue or MLE-12 cells were sonicated in Trizol reagent (Life Technologies, USA) and then homogenized according to the manufacturer's protocol. After integrity and purity determination, about 1 μg of RNA was then applied to reverse cDNA with a PrimeScript II cDNA Kit (Vazyme, China). Subsequently, the qPCR detection protocol utilized an SYBR Premix II kit (Vazyme, China). Primer sequences are listed in Table 1.

Western Blotting Analysis

Mouse lung tissues or cells were lysed using RIPA lysis buffer containing the protein inhibitor mixture. Total protein concentrations were quantified using the BCA kit (Thermo Fisher Scientific). Samples were denatured at 100 °C for 10 min and separated on 10–15% SDS-PAGE gels with standard molecular weights. Proteins from SDS-pAGE gels were transferred to PVDF membranes (Merck Millipore, Darmstadt), blocked with 5% skim milk for 2 h, and incubated with

Table 1 Primers Used for qRT- PCR Analysis

Genes	Primer sequences (5′–3′)
IL- 1β- F	TTCCTTGTGCAAGTGTCTGAAG
IL- 1β- R	CACTGTCAAAAGGTGGCATTT
IL- 6- F	CTCCGCAAGAGACTTCCAG
IL- 6- R	GGTCTGTGTGTGTGGGTGGTATC
TNF-α- F	TTCTCATTCCTGCTTGTGG
TNF-α- R	ACTTGGTGGTTTGCTACG
xCT- F	GGCACCGTCATCGGATCAG
xCT- R	CTCCACAGGCAGACCAGAAAA
GPX4- F	GATGGAGCCCATTCCTGAACC
GPX4- R	CCCTGTACTTATCCAGGCAGA
NOX1- F	GGTTGGGGCTGAACATTTTTC
NOX1- R	TCGACACACAGGAATCAGGAT
ACSL4- F	CTCACCATTATATTGCTGCCTGT
ACSL4- R	TCTCTTTGCCATAGCGTTTTTCT
NRF2- F	TCTTGGAGTAAGTCGAGAAGTGT
NRF2- R	GTTGAAACTGAGCGAAAAAGGC
PTGS2- F	TTCAACACACTCTATCACTGGC
PTGS2- R	AGAAGCGTTTGCGGTACTCAT
GAPDH- F	CTITGGCATTGTGGAAGGGC
GAPDH- R	CAGGGATGATGTTCTGGGCA

https://doi.org/10.2147/JIR.S520404

the primary antibodies overnight at 4 °C. After three washes, the membranes were incubated with the corresponding HRP-conjugated secondary antibody (1:5000, Proteintech, Wuhan, China) for 1 h at room temperature. Protein bands were detected using ECL, ImageJ software was used to analyze the intensity of protein bands in the realistic images. The band intensities of the photonic crystals were analyzed using ImageJ software.

Measurement of Ferroptosis-Related Markers

The levels of Fe^{2+}, malondialdehyde (MDA) and reduced glutathione (GSH) in alveolar epithelial cells were detected by iron detection kit that all detection kits were from Nanjing Jianxian Bioengineering Institute. The reactive oxygen species (ROS) detection kit was also from Nanjing Jianxian Bioengineering Institute.

Database Source

The target genes of melatonin were screened from the TCMSP database, and the BPD genes obtained from GeneCards were intercrossed to obtain the key genes (http://www.genecards.org/). The molecular docking model between melatonin and KEAP1 was obtained by Autodock and Pymol software.

Molecular Docking Prediction

To assess the potential binding affinity between Melatonin and the KEAP1 protein, we employed molecular docking technology. Initially, the compound's structure in the mol2 format was obtained directly from the TCMSP tool. Subsequently, crystal structures of the candidate proteins were acquired from the RCSB PDB database (www.rcsb.org),[30] and these structures underwent ligand and water molecule removal using PyMOL software. Molecular docking was then performed utilizing the Swissdock tool, and the results were imported into UCSF Chimera 1.14 software for visualization and analysis.

Statistical Analysis

All data were expressed as mean ± S.E. One-way and two way analysis of variance (ANOVA) techniques were used for data analysis of more than two groups followed by GraphPad Prism analysis. A value of $P < 0.05$ was considered statistically significant.

Result

Melatonin Attenuates Hyperoxia-Induced BPD

In this study, we established a mouse model of BPD by exposure to hyperoxia,[14] and further investigated the protective effect of MT on BPD mice and its mechanism (Figure 1A). In our study, we noted that neonatal mice lost weight after 14 days of hyperoxia compared with the air environment (CON group). Hematoxylin-eosin (HE) staining showed that after hyperoxia exposure, the alveoli in the lung tissue of mice were severely damaged, the structure was disordered, the shape was extremely irregular, and the number was significantly reduced. As for the mice exposed to hyperoxia were treated with MT at the same time, the number of alveoli was increased, the shape of alveoli was improved (Figure 1B). However, when the hyperoxia exposed mice were treated with MT at the same time (HYP+MT group), the body weight recovered significantly, reaching 83.5% of that of the CON group (Figure 1C), the radial alveolar count (RAC) was significantly increased (Figure 1D), and the mean alveolar intercept (MLI) was significantly reduced (Figure 1E). Compared with the control group, the levels of inflammatory factors interleukin (IL)-1β, IL-6 and TNF-α mRNA in the lung tissues of the model group were up-regulated. Compared with the model group, the mRNA levels of inflammatory factors IL-1β, IL-6 and TNF-α in lung tissue of MT-treated mice were down-regulated (Figure 1F–H). The mRNA levels of inflammatory factors IL-1β, IL-6 and TNF-α in lung epithelial cells (MLE-12) cultured in 85% hyperoxia were increased, and the mRNA levels were down-regulated after MT treatment. (Supplementary Figure 1A–C). These results indicate that MT attenuates hyperoxia induced lung injury in mice.

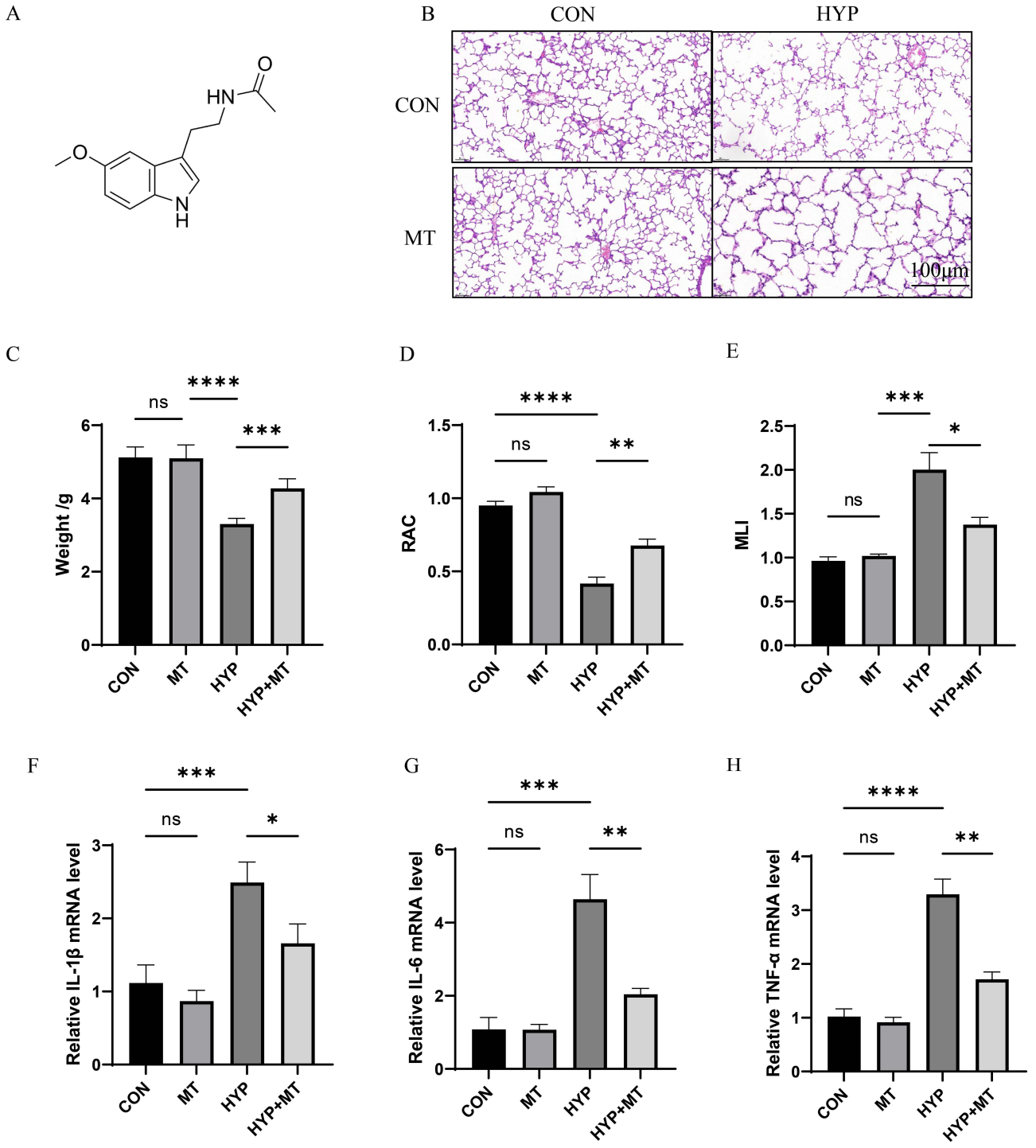

Figure 1 Melatonin attenuates hyperoxia-induced lung injury. (**A**) Molecular structure of melatonin (**B**) HE staining of lung tissue in mice (**C**) Body weight of mice (**D**) Radial alveolar count of lung tissue in mice (**E**) Mean linear intercept of lung tissue in mice (**F–H**) mRNA levels of IL-1β, IL-6 and TNF-α in lung tissue of mice. Data are expressed as mean ± SD (n = 5), **p* < 0.05, ***p* < 0.01, ****p* < 0.001, *****p* < 0.0001 indicate significant differences from each group.

Melatonin Inhibits Ferroptosis in BPD

To understand the effect of MT on ferroptosis in hyperoxia induced BPD, we examined the ferroptosis marker proteins GPX4, xCT, NADPH oxidase 1(NOX1), and Acyl Coenzyme A Synthetase Long Chain Family, Member 4(ACSL4) The results showed that the levels of GPX4 and xCT mRNA in the lung tissue of MT treatment group (HYP + MT) were significantly increased (Figure 2A and B), and the levels of NOX1 and ACSL4 mRNA were significantly decreased

https://doi.org/10.2147/JIR.S520404

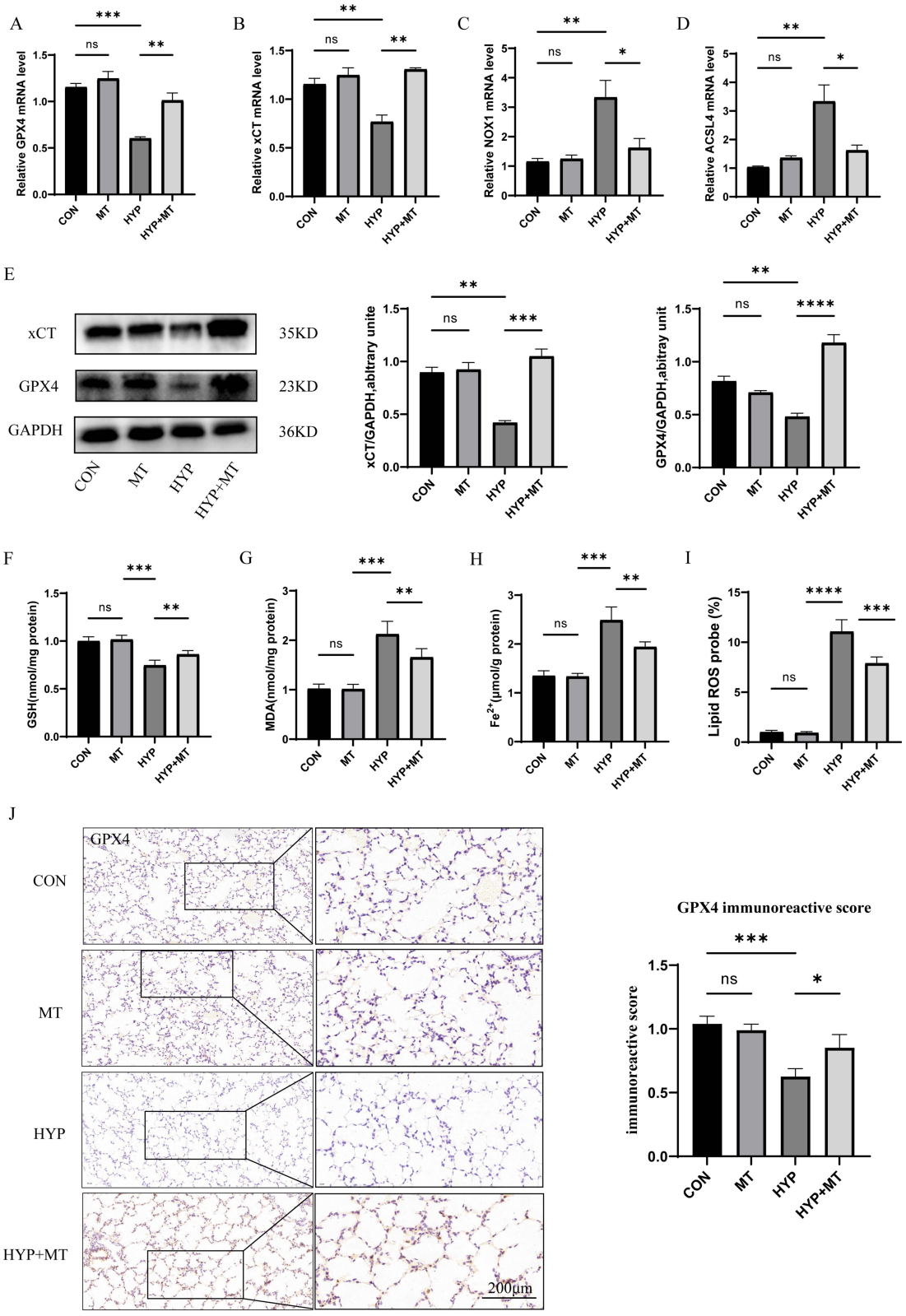

Figure 2 Melatonin inhibits ferroptosis in BPD. (**A**–**D**) mRNA levels of ferroptosis marker proteins GPX4, xCT, NOX1 and ACSL4 in lung tissue of mice. (**E**) protein levels of GPX4 and xCT in lung tissue of mice and their quantitative analysis. (**F**–**I**) detection of GSH, MDA, Fe^{2+} and lipid ROS kits in lung tissue of mice. (**J**) immunohistochemical detection and quantitative analysis of lung tissue of mice. *$p < 0.05$, **$p < 0.01$; ***$p < 0.001$, ****$p < 0.0001$ indicate significant differences from each group.

(Figure 2C and D) compared with these in the hyperoxia group. In alveolar epithelial cells, compared with the hyperoxia group, the changes of GPX4, xCT, NOX1 and ACSL4 mRNA levels after MT treatment (HYP + MT) were the same as those in the lung tissue of mice (Supplementary Figure 2A–D). Then, we detected the protein levels of GPX4 and xCT. Compared with the hyperoxia group, GPX4 and xCT protein levels were significantly increased after MT treatment (Figure 2E). The same protein trend was observed at the cellular level (Supplementary Figure 2E). After that, we measured the levels of glutathione (GSH), Malondialdehyde (MDA), Fe^{2+} and Reactive Oxygen Species (ROS). In the lung tissue of mice, hyperoxia increased the contents of ROS, MDA and Fe^{2+} and decreased the content of GSH (Figure 2F–I). However, MT treatment significantly reduced the content of ROS, MDA and Fe^{2+} induced by hyperoxia, and increased the content of GSH. Immunohistochemistry showed that the positive rate of GPX4 reduced after hyperoxia, which could be reversed after MT treatment (Figure 2J). By immunofluorescence staining of lung tissue sections and alveolar epithelial cells, the results showed that similar to immunohistochemistry, the expression of GPX4 in the hyperoxia group was reduced, and MT could reverse this increase (Supplementary Figure 2F and G).

Erastin Abolished the Effect of Melatonin on MLE-12 Cells in Hyperoxia Conditions

In order to further explore the impact of MT on ferroptosis, we treated MLE-12 cells prior to exposed to MT with erastin, an inducer of ferroptosis. The results indicated that compared to the HYP+MT group, the levels of GPX4 and xCT in the HYP+MT+Erastin group were significantly reduced (Figure 3A and B), while prostaglandin-endoperoxide synthase 2 (PTGS2) levels were notably increased (Figure 3C). Western blot analysis showed that GPX4 and xCT protein expression in the HYP+MT+Erastin group exhibited a similar trend as mRNA levels compared to the HYP+MT group (Figure 3D). Subsequently, ROS was assessed. In MLE-12 cells, treatment with erastin reversed the impact of MT treatment on high oxygen-induced oxidative stress (Figure 3E).

Melatonin Can Improve BPD by Inhibiting Ferroptosis via Activating KEAP1/NRF2/PTGS2 Signaling Pathway

Molecular docking between melatonin and the NRF2-binding protein KEAP1 showed that melatonin could bind to KEAP1, thereby activating NRF2 nuclear translocation and inhibiting ferroptosis, thus providing a protective effect. The binding energy of the most stable structure obtained using Autodock4 docking was −6.4 kcal/mol. The primary docking site is that the hydroxyl group of melatonin forms two hydrogen bonds with residues Ile559, Ile416, Val512, Val463, Ala336, Leu365, Arg415, Gly462 and Gly509 of KEAP1 protein, with the main contributions to binding being van der Waals interactions, hydrogen bonding, and desolvation energy (Figure 4A). According to the molecular docking results in this study, melatonin can directly inhibit the function of KEAP1, possibly destroy the stability of KEAP1- NRF2 complex, reduce the ubiquitination and degradation of NRF2, and lead to the accumulation of NRF2. By immunofluorescence confocal microscopy, we found that KEAP1-NRF2 complex was decreased and NRF2 was accumulated after melatonin treatment compared with the normal group (Supplementary Figure 3). The related targets of melatonin and BPD were obtained by screening the Chinese Medicine System Pharmacology Database and Analysis Platform (TCMSP) database and GeneCard database, among which PTGS2 was the key gene. PPI network showed that KEAP1 affected NFE2L2 and possibly PTGS2. (Figure 4B and C).

Subsequently, the hyperoxia group showed a decrease in NRF2 level and an increase in KEAP1 and PTGS2 levels as determined by Western blot compared with the control group, and the protein level of NRF2 increased and KEAP1 and PTGS2 decreased after MT treatment (Figure 4D and E). The immunofluorescence trends for NRF2 and PTGS2 in mouse lung tissue were similar to those for protein levels (Figure 4F and G). MT may affect the expression of ferroptosis key protein PTGS2 by promoting NRF2 expression and decreasing KEAP1 expression to inhibit ferroptosis in MLE-12 cells.

ML385 Abolished the Effect of Melatonin on MLE-12 Cells in Hyperoxia

To investigate the role of NRF2 in the effects of MT on MLE-12 cells, MT-treated MLE-12 cells were treated with hyperoxia and the NRF2 inhibitor ML385. In the HYP+MT group cells treated with ML385, the mRNA and protein

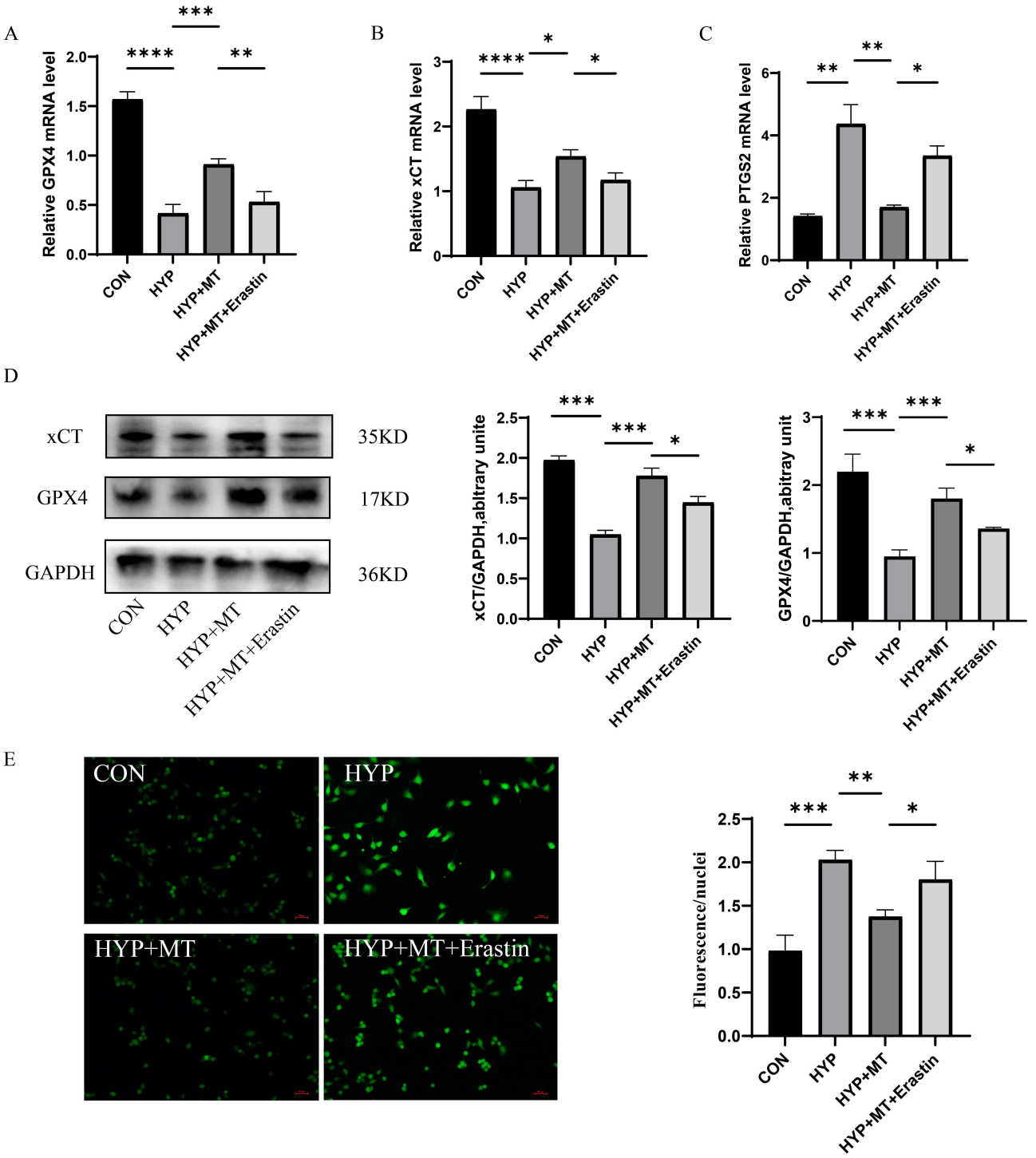

Figure 3 Erastin abolished the effect of melatonin on MLE-12 cells under hyperoxia condition. (**A–C**) mRNA levels of ferroptosis marker genes GPX4, xCTand PTGS2 in MLE-12 cells. (**D**) protein levels of GPX4 and xCT in MLE-12 cells and their quantitative analysis. (**E**) Reactive oxygen species detection and fluorescence intensity analysis. *$p < 0.05$, **$p < 0.01$; ***$p < 0.001$, ****$p < 0.0001$ indicate significant differences from each group.

levels of NRF2, GPX4, and xCT were decreased, and those of KEAP1, PTGS2 were increased (Figure 5A–D), which reversed the protective effect of MT. In addition, ML385 treatment reversed the increase in cell viability and decrease in inflammation in MT-treated cells (Figure 5E and F). Similarly, ML385 treatment effectively reversed the decrease in intracellular ROS after MT treatment (Figure 5G). Together, these findings suggest that the KEAP1/NRF2/PTGS2 axis is important in mediating the effects of MT on MLE-12 cells.

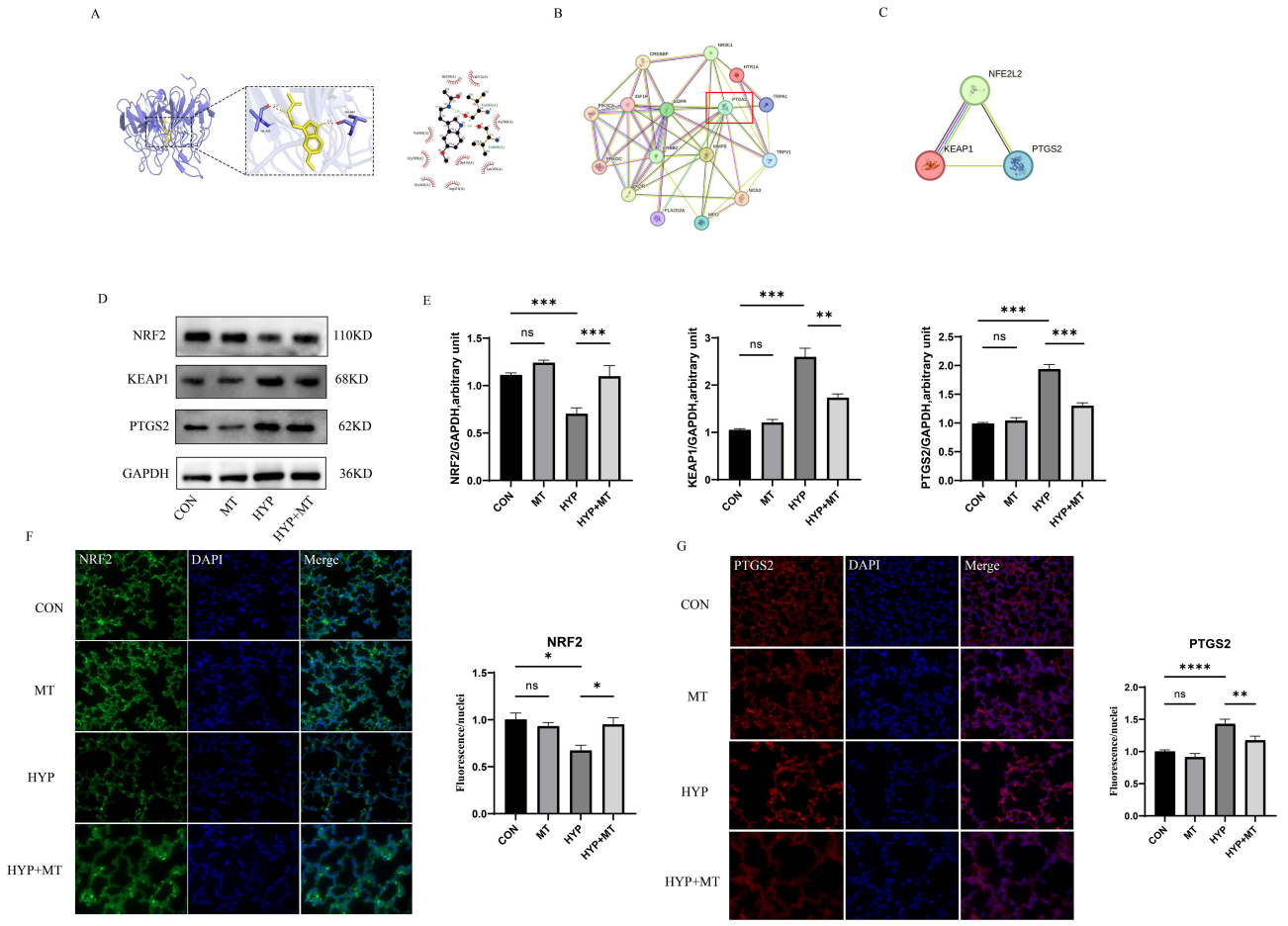

Figure 4 Melatonin can improve BPD by inhibiting ferroptosis by activating KEAP1/NRF2/PTGS2 signaling pathway. (**A**) Molecular docking prediction of Melatonin and KEAP1. (**B**)STRING analysis of the related targets of BPD and melatonin. (**C**) Interactions between KEAP1, PTGS2, and NFE2L2. (**D** and **E**) protein levels of KEAP1, NRF2 and PTGS2 in lung tissue of mice and their quantitative analysis. (**F** and **G**) Immunofluorescence and fluorescence intensity analysis of NRF2 and PTGS2 in lung tissues of mice. *p < 0.05, **p < 0.01; ***p < 0.001, ****p < 0.0001 indicate significant differences from each group.

Discussion

Significant advancements in neonatal medicine have improved the survival and prognosis of preterm infants with low gestational age; however, recurrent oxygen therapy increases the risk of hyperoxic lung injury and secondary BPD. Despite the clinical application of numerous novel pharmacological agents, BPD remains neither preventable nor curable. BPD is a multifactorial disorder, with oxidative stress induced by hyperoxia being the most prominent contributor.[31,32] Disruption of systemic oxidative homeostasis can trigger diverse forms of regulated cell death, including ferroptosis—an iron-dependent programmed cell death driven by lipid peroxidation. Previous studies have demonstrated ferroptosis involvement in hyperoxic lung injury in neonatal rats.[13,33] Our study revealed ferroptosis-like alterations in both alveolar epithelial cells and pulmonary tissue of BPD mice exposed to hyperoxia, characterized by elevated Fe^{2+}, ROS, and MDA levels, upregulated expression of GPX4, xCT, NOX1, and ACSL4 genes, and reduced GSH, a critical antioxidant.

MT has been reported to mitigate ferroptosis in multiple pathologies. For instance, MT alleviates sepsis-induced acute respiratory distress syndrome (ARDS) by suppressing NCOA4-mediated ferritinophagy in alveolar macrophages.[21] In this study, MT administration attenuated hyperoxia-induced ROS, MDA, and Fe^{2+} accumulation while restoring GSH levels. Melatonin effectively suppressed both inflammatory responses and ferroptosis in pulmonary tissue and alveolar epithelial cells (MLE-12) of hyperoxia-exposed mice. Furthermore, prior studies highlight the pivotal role of NRF2 in mediating lipid peroxidation and ferroptosis.[34–37] Activation of the NRF2/HO-1 axis ameliorates hyperoxia-induced acute lung injury by inhibiting ferroptosis.[38] Notably, xCT and GPX4 are central regulators of ferroptosis, while PTGS2

https://doi.org/10.2147/JIR.S520404

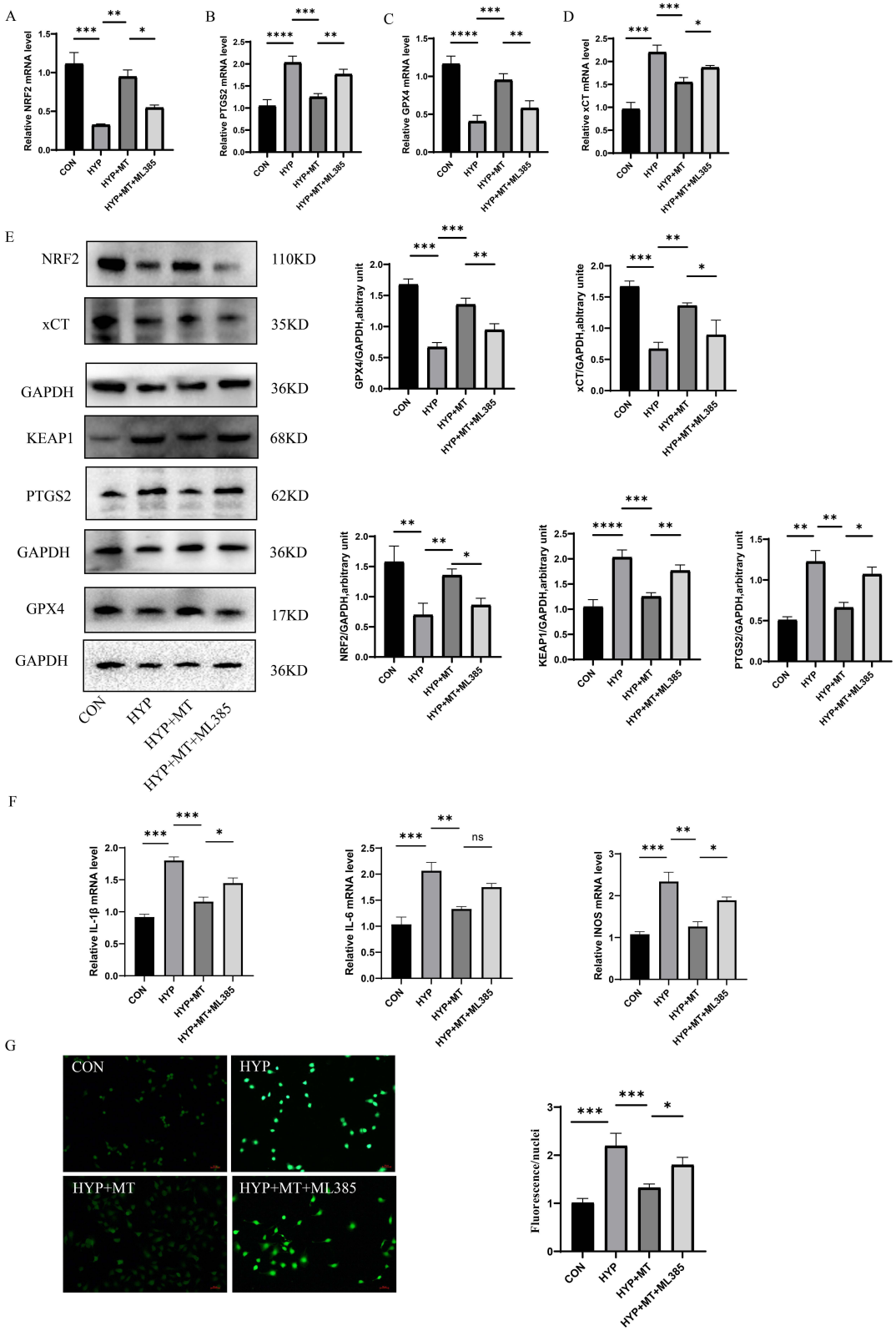

Figure 5 ML385 abolished the effect of melatonin on MLE-12 cells under hyperoxia. (**A**–**D**) mRNA levels of NRF2, PTGS2, xCT and GPX4 in MLE-12 cells. (**E**) protein levels of NRF2, KEAP1, PTGS2, GPX4 and xCT in MLE-12 cells and their quantitative analysis. (**F**) mRNA levels of IL-1β,IL-6 and TNF-αin MLE-12 cells.(**G**) Reactive oxygen species detection and fluorescence intensity analysis. *$p < 0.05$, **$p < 0.01$; ***$p < 0.001$, ****$p < 0.0001$ indicate significant differences from each group.

serves as a biomarker of this process.[39] Thus, the KEAP1/NRF2/PTGS2 pathway may constitute a key mechanism through which MT inhibits ferroptosis and protects against BPD.

Our findings demonstrate that MT treatment activates NRF2 expression and suppresses PTGS2 expression, effects reversible by the ferroptosis inducer Erastin. This suggests that melatonin's protective effects in hyperoxia-induced BPD animal models are mediated via ferroptosis inhibition in vitro and in vivo. Melatonin reversed hyperoxia-induced reductions in NRF2, GPX4, and xCT levels, while downregulating KEAP1 and PTGS2 expression. Concurrently, the NRF2 inhibitor ML385 abolished MT's protective effects against hyperoxia-induced ferroptosis and inflammation in pulmonary epithelial cells.

In summary, we demonstrate that melatonin protects alveolar epithelial cells and neonatal mice from hyperoxia-induced ferroptosis by activating the KEAP1/NRF2/PTGS2 axis, thereby attenuating hyperoxic lung injury and fetal growth restriction. Although further investigation is warranted, our results identify melatonin as a potential therapeutic strategy for preventing and treating ferroptosis-associated BPD.

Abbreviations

BPD, bronchopulmonary dysplasia; GPX4, glutathione peroxidase 4; SPC, synthesize surfactant protein C; ROS, reactive oxygen species; FTH1, ferritin heavy chain 1; SLC7A11, solute carrier family 7 member 11; HIF-1α, Hypoxia inducible factor 1, alpha; VEGF, vascular endothelial growth factor; NRF2, nuclear factor erythroid 2-related factor 2; HO-1, Heme Oxygenase-1; KEAP1, Kelch-like ECH associated protein-1; SOD, superoxide dismutase.

Data Sharing Statement

The data used during the current study are available from the corresponding author upon reasonable request. The all data is available from Xianhui Deng.

Ethics Approval and Consent to Participate

The experimental procedure was approved by the committee of the experimental animal protection and use committee of Jiangnan University JN.No20240315c0180630[108]. We have adhered to ARRIVE guidelines and upload a completed checklist or provide links.

Author Contributions

All authors made a significant contribution to the work reported, whether that is in the conception, study design, execution, acquisition of data, analysis and interpretation, or in all these areas; took part in drafting, revising or critically reviewing the article; gave final approval of the version to be published; have agreed on the journal to which the article has been submitted; and agree to be accountable for all aspects of the work.

Funding

This work was supported by the National Natural Science Foundation of China (No. 82101812), the Jiangsu Provincial Commission of Health and Family Planning (No. Z2020042), and the Medical Key Discipline Program of Wuxi Health and Family Planning Commission (No. CXTD202113), and the Scientific research project of Wuxi Municipal Health Commission (No.M202414).

Disclosure

The authors report no conflicts of interest in this work.

References

1. Thomas JM, Sudhadevi T, Basa P, et al. The role of sphingolipid signaling in oxidative lung injury and pathogenesis of bronchopulmonary dysplasia. *Int J Mol Sci*. 2022;23:1254. doi:10.3390/ijms23031254
2. Deng X, Bao Z, Yang X, et al. Molecular mechanisms of cell death in bronchopulmonary dysplasia. *Apoptosis*. 2023;28:39–54. doi:10.1007/s10495-022-01791-4

3. Wu T-J, Jing X, Teng M, et al. Role of myeloperoxidase, oxidative stress, and inflammation in bronchopulmonary dysplasia. *Antioxidants*. 2024;13:889. doi:10.3390/antiox13080889
4. Shahzad T, Dong Y, Behnke NK, et al. Anti-CCL2 therapy reduces oxygen toxicity to the immature lung. *Cell Death Discov*. 2024;10:311. doi:10.1038/s41420-024-02073-5
5. Menegolla MP, Silveira RC, Görgen ARH, et al. Antibiotics and beyond: unraveling the dynamics of bronchopulmonary dysplasia in very preterm infants. *Pediatr Pulmonol*. 2024;59:3260–3267. doi:10.1002/ppul.27182
6. van de Loo M, van Kaam A, Offringa M, et al. Corticosteroids for the prevention and treatment of bronchopulmonary dysplasia: an overview of systematic reviews. *Cochrane Database Syst Rev*. 2024:4:CD013271. doi:10.1002/14651858.CD013271.pub2
7. Manley BJ, Cripps E, Dargaville PA. Non-invasive versus invasive respiratory support in preterm infants. *Semin Perinatol*. 2024;48:151885. doi:10.1016/j.semperi.2024.151885
8. Jain KG, Liu Y, Zhao R, et al. Humanized L184Q mutated surfactant protein c gene alters alveolar type 2 epithelial cell fate. *Int J Mol Sci*. 2024;25:8723. doi:10.3390/ijms25168723
9. Zhu H, Zhang R, Bao T, et al. Interleukin-11 is involved in hyperoxia-induced bronchopulmonary dysplasia in newborn mice by mediating epithelium-fibroblast cross-talk. *Inflammation*. 2024. doi:10.1007/s10753-024-02089-0
10. Abdel LM, Davis PG, Wheeler KI, et al. Surfactant therapy via thin catheter in preterm infants with or at risk of respiratory distress syndrome. *Cochrane Database Syst Rev*. 2021;5(5):CD011672. doi:10.1002/14651858.CD011672
11. Yang J, Zhang M, Zhang X, et al. Glioblastoma-derived exosomes promote lipid accumulation and induce ferroptosis in dendritic cells via the NRF2/GPX4 pathway. *Front Immunol*. 2024;15:1439191. doi:10.3389/fimmu.2024.1439191
12. Kan S, Feng S, Zhao X, et al. UAMC-3203 inhibits ferroptosis and promotes functional recovery in rats with spinal cord injury. *Sci Rep*. 2024;14:20180. doi:10.1038/s41598-024-70926-1
13. Yang M, Chen Y, Huang X, et al. ETS1 ameliorates hyperoxia-induced bronchopulmonary dysplasia in mice by activating Nrf2/HO-1 mediated ferroptosis. *Lung*. 2023;201:425–441. doi:10.1007/s00408-023-00639-1
14. Zhu Y, Hou H, Li Y, et al. Hyperoxia exposure induces ferroptosis and apoptosis by downregulating PLAGL2 and repressing HIF-1α/VEGF signaling pathway in newborn alveolar typeII epithelial cell. *Redox Rep*. 2024;29:2387465. doi:10.1080/13510002.2024.2387465
15. Deng X, Chen D, Xie A, et al. Quercetin alleviates hyperoxia-induced bronchopulmonary dysplasia by inhibiting ferroptosis through the MAPK/PTGS2 pathway: insights from network pharmacology, molecular docking, and experimental evaluations. *Chem Biol Drug Des*. 2024;103:e14520. doi:10.1111/cbdd.14520
16. Chen D, Gao ZQ, Wang YY, et al. Sodium propionate enhances Nrf2-mediated protective defense against oxidative stress and inflammation in lipopolysaccharide-induced neonatal mice. *J Inflamm Res*. 2021;14:803–816. doi:10.2147/JIR.S303105
17. Mukherjee U, Sehar U, Brownell M, Reddy PH. Mechanisms, Consequences and Role of Interventions for Sleep Deprivation: focus on Mild Cognitive Impairment and Alzheimer's Disease in Elderly. *Ageing Res Rev*. 2024;100:102457. doi:10.1016/j.arr.2024.102457
18. Tao Z-S, Hu X-F, Sun T. Melatonin prevents bone loss in osteoporotic rats with valproic acid treatment by anti-inflammatory and anti-oxidative stress. *Int Immunopharmacol*. 2024;141:112932. doi:10.1016/j.intimp.2024.112932
19. Cinar D, Altinoz E, Elbe H, et al. Therapeutic effect of melatonin on CCl4-induced fibrotic liver model by modulating oxidative stress, inflammation, and TGF-β1 signaling pathway in pinealectomized rats. *Inflammation*. 2024. doi:10.1007/s10753-024-02101-7
20. Jung KH, Kim SE, Go HG, et al. Synergistic renoprotective effect of melatonin and zileuton by inhibition of ferroptosis via the AKT/mTOR/NRF2 signaling in kidney injury and fibrosis. *Biomol Ther*. 2023;31:599–610. doi:10.4062/biomolther.2023.062
21. Xu W, Wu Y, Wang S, et al. Melatonin alleviates septic ARDS by inhibiting NCOA4-mediated ferritinophagy in alveolar macrophages. *Cell Death Discov*. 2024;10:253. doi:10.1038/s41420-024-01991-8
22. Yu X, Wang S, Wang X, et al. Melatonin improves stroke by inhibiting autophagy-dependent ferroptosis mediated by NCOA4 binding to FTH1. *Exp Neurol*. 2024;379:114868. doi:10.1016/j.expneurol.2024.114868
23. Jing X, Chen Z, Zhang M, et al. Melatonin mitigates the lipopolysaccharide-induced myocardial injury in rats by blocking the p53/xCT pathway-mediated ferroptosis. *Naunyn Schmiedebergs Arch Pharmacol*. 2024;398:1653–1663. doi:10.1007/s00210-024-03367-2
24. He F, Wang Q-F, Li L, et al. Melatonin protects against hyperoxia-induced apoptosis in alveolar epithelial type II cells by activating the MT2/PI3K/AKT/ETS1 signaling pathway. *Lung*. 2023;201:225–234. doi:10.1007/s00408-023-00610-0
25. Pavlyshyn H, Sarapuk I, Kozak K. The relationship of melatonin concentration in preterm infants and adverse outcomes in the late neonatal period. *Biochem Med*. 2023;33:010706. doi:10.11613/BM.2023.010706
26. Pan L, Fu J-H, Xue X-D, et al. Melatonin protects against oxidative damage in a neonatal rat model of bronchopulmonary dysplasia. *World J Pediatr*. 2009;5:216–221. doi:10.1007/s12519-009-0041-2
27. Suleymanoglu S, Cekmez F, Cetinkaya M, et al. Protective effects of melatonin therapy in model for neonatal hyperoxic lung injury. *Altern Ther Health Med*. 2014;20:24–29.
28. Salmanoglu DS, Gurpinar T, Vural K, et al. Melatonin and L-carnitin improves endothelial disfunction and oxidative stress in Type 2 diabetic rats. *Redox Biol*. 2016;8:199–204. doi:10.1016/j.redox.2015.11.007
29. Chen X-Q, Wu S-H, Luo -Y-Y, et al. Lipoxin A4 attenuates bronchopulmonary dysplasia via upregulation of Let-7c and downregulation of TGF-β1 signaling pathway. *Inflammation*. 2017;40:2094–2108. doi:10.1007/s10753-017-0649-7
30. Burley SK, Bhikadiya C, Bi C, et al. RCSB protein data bank (RCSB.org): delivery of experimentally-determined PDB structures alongside one million computed structure models of proteins from artificial intelligence/machine learning. *Nucleic Acids Res*. 2023:51:D488–D508. doi:10.1093/nar/gkac1077
31. Giusto K, Wanczyk H, Jensen T, Finck C. Hyperoxia-induced bronchopulmonary dysplasia: better models for better therapies. *Dis Model Mech*. 2021;14:dmm047753. doi:10.1242/dmm.047753
32. Dankhara N, Holla I, Ramarao S, Kalikkot Thekkeveedu R. Bronchopulmonary dysplasia: pathogenesis and pathophysiology. *J Clin Med*. 2023;12:4207. doi:10.3390/jcm12134207
33. Chou H-C, Chen C-M. Cathelicidin attenuates hyperoxia-induced lung injury by inhibiting ferroptosis in newborn rats. *Antioxidants*. 2022;11:2405. doi:10.3390/antiox11122405
34. Li X, Qian J, Xu J, et al. NRF2 inhibits RSL3 induced ferroptosis in gastric cancer through regulation of AKR1B1. *Exp Cell Res*. 2024;442:114210. doi:10.1016/j.yexcr.2024.114210

35. Han Z, Wang B, Wen Y-Q, et al. Acteoside alleviates lipid peroxidation by enhancing Nrf2-mediated mitophagy to inhibit ferroptosis for neuroprotection in Parkinson's disease. *Free Radic Biol Med*. 2024;S0891-5849(24):00564. doi:10.1016/j.freeradbiomed.2024.07.018
36. Li K, Wang X-Q, Liao Z-L, et al. Wedelolactone inhibits ferroptosis and alleviates hyperoxia-induced acute lung injury via the Nrf2/HO-1 signaling pathway. *Toxicol Sci*. 2024:kfae099. doi:10.1093/toxsci/kfae099
37. Li X, Wu L, Sun L, et al. Ferroptosis-related gene signatures in epilepsy: diagnostic and immune insights. *Mol Neurobiol*. 2024. doi:10.1007/s12035-024-04385-0
38. Zhu X, Han X, Wang J. Sufentanil-induced Nrf2 protein ameliorates cerebral ischemia-reperfusion injury through suppressing neural ferroptosis. *Int J Biol Macromol*. 2024;279:135109. doi:10.1016/j.ijbiomac.2024.135109
39. Zhao G, Liu Y, Wei X, et al. Identification of penexanthone a as a novel chemosensitizer to induce ferroptosis by targeting nrf2 in human colorectal cancer cells. *Mar Drugs*. 2024;22:357. doi:10.3390/md22080357